

INDISTINGUISHABLE SINGLE PHOTONS FROM COUPLE NANO-CAVITIES

CARLOS G. SEVILLA¹ AND ABHI SAXENA² AND ARKA MAJUMDAR^{2,3}

ABSTRACT

The production of indistinguishable single photons is a pre-requisite for the achievement of quantum computing. However, the indistinguishability of available bare quantum emitters is far from unity. Based on our paper of improving indistinguishability from colloidal quantum dots (1), we here discuss the improved indistinguishability of bare quantum emitters using the method of coupled cavities. We then suggest a viable, experimental design, also from our paper (1), utilizing colloidal quantum dots and compare results with those of other quantum emitters.

Keywords: Indistinguishable single photon source, Colloidal quantum dots

1. INTRODUCTION

Developing methods for the generation of indistinguishable single photons is a stepping stone towards universal quantum computing (2). Single indistinguishable photons have garnered considerable attention as a candidate for quantum computing qubits. However, currently available quantum emitters QEs suffer from low indistinguishability. For a bare quantum emitter, indistinguishability I is given as (3)

$$I = \frac{\gamma}{\gamma + \gamma^*} \quad (1)$$

where γ is the radiative decay rate and γ^* the pure dephasing rate of our quantum emitter. Due to local environmental conditions $\gamma^* \gg \gamma$ for a bare emitter. For colloidal quantum dots QDs, and at room temperature this can be $\gamma^* \approx \gamma$, giving us a $I \approx 10^{-5}$ (4)

Several methods to improve I of these emitters have been suggested, such as spectral filtering and coupling to an optical cavity (5), however, these methods see a large decrease in the efficiency β of these emitters. A newly suggested method utilizing the successive coupling of two separate optical cavities has been shown to both decrease the emission line width, thus increasing output I , as with a single photon, and improve β , as compared to other methods (5). In this paper we examine the viability of this new method with reference to an experimentally feasible design proposed in our previous paper (1).

2. SYSTEM OF COUPLED CAVITIES

Our system, modelled by a common Jaynes-Cummings Hamiltonian (6), consists of a single quantum emitter coupled to a first cavity, denoted c_1 , and this subsystem then coupled to a second cavity c_2 . The Hamiltonian for our system is thus denoted

$$H = \omega_e e^\dagger e + \omega_e c_1^\dagger c_1 + \omega_e c_2^\dagger c_2 + g(e^\dagger c_1 + e c_1^\dagger) + J(c_1^\dagger c_2 + c_1 c_2^\dagger)$$

Here e^\dagger , e and c_i are the corresponding creation and annihilation operators for our emitter and cavities. Like-

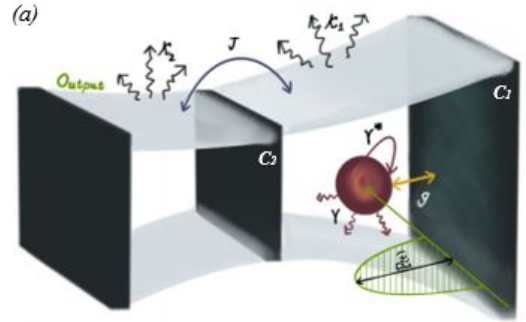


Figure 1. Graphical Illustration of a quantum emitter coupled to successive cavities

wise g and J denote the coupling coefficients between our emitter and c_1 and between c_1 and c_2 respectively and finally ω_e our bare emitter's emission frequency, where we have assumed all cavities are on resonance.

A graphical representation of our system can be seen in Fig 1, where we have additionally denoted k_1 and k_2 as the decay rates of our corresponding cavities.

Methodically, our system is initiated by a pulse laser, also on resonance, which raises our emitter to an excited state. Then after a subsequent decay, the emitted photon will have some probability, dependent on g , to enter c_1 . From here, our photon will have a similar probability of proceeding to the second cavity, dependent on J and k_1 . Finally, our emitted photon can pass into the output, dependent on k_2 , where it is measured.

Our system is then simulated using the evolution of its corresponding density matrix, according to the master equation (7). It has then be shown that indistinguishability I is given as (3)

$$I = \frac{\int_0^\infty dt \int_0^\infty d\tau |\langle c_2^\dagger(t+\tau)c_2(t) \rangle|}{\int_0^\infty dt \int_0^\infty d\tau \langle c_2^\dagger(t)c_2(t) \rangle \langle c_2^\dagger(t+\tau)c_2(t+\tau) \rangle}$$

And likewise, efficiency β

$$\beta = k_2 \int_0^\infty \langle c_2^\dagger(t)c_2(t) \rangle dt$$

¹ School of Natural Sciences, Hampshire College, Amherst, MA, 01002

² Electrical and Computer Engineering, University of Washington, Seattle, WA, 98195

³ Department of Physics, Univeristy of Washington, Seattle, WA, 98195

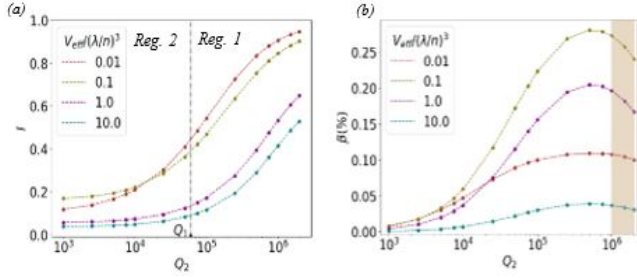


Figure 2. Plots for four different values of V_{eff} . a) I as a function of Q_2 . b) β as a function of Q_2 . Where $Q_2 = 6 * 10^4$ and $J = 2.1\gamma$

3. PARAMETER ANALYSIS

The ability of an optical cavity to increase the indistinguishability of our incident photons is dictated by their ability to narrow their associated line width Γ , usually indicated by a cavity's Quality Factor $Q = \frac{\omega}{\Gamma} = \frac{\omega}{k}$.

Our optical cavities are produced with an associated and related Q and cavity mode volume V_{eff} . It goes to reason that our output's I and β benefit from the highest feasible g since this will determine if our emitted photons will proceed to our coupled cavities. Our coupling g is inversely proportional to $\sqrt{V_{eff}}$ (8), meaning our mode volume of our first cavity should be minimized and quality factor of our first cavity Q_1 is largely limited. Therefore, the two degrees of freedom we are predominantly interested in are the quality factor of our second cavity Q_2 and our second coupling coefficient J .

To thoroughly examine changes in these two parameters, we must additionally define the corresponding transfer rates (3)

$$R_1 = \frac{4g^2}{\gamma + \gamma^* + k_1}; \quad R_2 = \frac{4j^2}{R_1 + k_1 + k_2} \quad (2)$$

where R_1 is the transfer rate from our emitter to c_1 and R_2 from c_1 to c_2

In Fig 2. we can see four plots for different values of mode volume. Our first graph of I as a function of Q_2 gives the expected result that as we increase the quality factor of our second cavity, so does our I , since increasing the quality factor of our cavity will increase its ability to decrease linewidth and thus enhance photon indistinguishability. Our second graph of β as a function of Q_2 also sees an increase in efficiency with the increase in quality factor. This is due to the simultaneous decrease in k_2 , which from equation(2) we see will increase R_2 and thus ensure photons successfully travel from our emitter to c_2 , and subsequently to our output.

This analysis is valid only within a regime where we see dominant unidirectional flow of photons. Otherwise, as R_2 increases we begin to observe considerable probability that a photon may incoherently jump from c_2 back to c_1 . We can see this in our plot as a noticeable decline in β within the shaded region.

In our second plots (Figure 3.), we see our same I and β now as functions of our coupling J . Our first graph of I is divided into a first region with near constant indistinguishability, where $R_2 < k_2$. In this regime, our system operates with photons passing through both cavities and experiencing the expected decrease in Γ . There is no noticeable change as we increase J and by extent R_2 until $R_2 > k_2$ in our second region. In this region

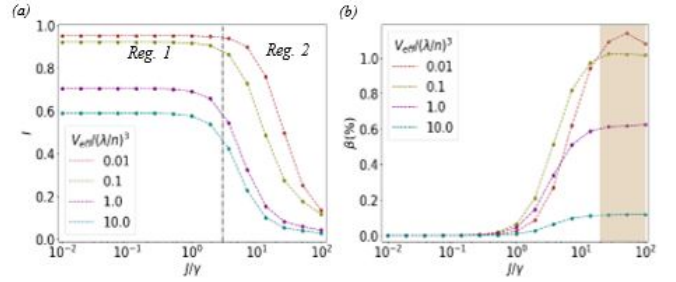


Figure 3. Plots of four different values of V_{eff} . a) I as a function of J . b) β as a function of J . Where $Q_1 = 6 * 10^4$ and $Q_2 = 2 * 10^6$ the transfer rate between c_1 and c_2 is large enough to interfere with unidirectional flow of photons and we begin to observe considerable jumping between cavities. This behaviour then causes a rapid decrease in I .

In our second graph for β we see an expected early increase in β as we increase J and by extent R_2 . This is due to an increased transfer rate from c_1 to c_2 and subsequently to our output. However, our β begins to suffer in the shaded region of our graph, where again we begin to see considerable photon jumping from c_2 back to c_1 .

From both of these simulated results we can optimize our parameters to achieve the highest possible joint I and β . Clearly we must achieve a high Q_2 , but not high enough that we see interrupted unidirectional flow of photons. Likewise, we need an intermediate J , before our I begins to dramatically decrease, but simultaneously after β has begun increasing. It turns out that this middle regime is approximately at the point where J is just larger than γ . Furthermore, from our plots the V_{eff} that performs best is between 0.1 and 1.

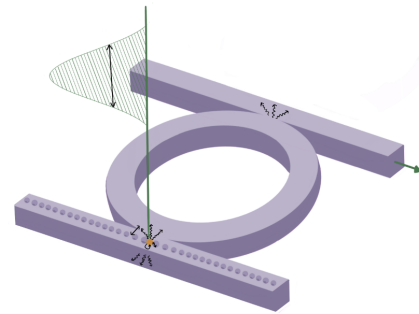


Figure 4. Design of the proposed experimental device. A SiN one dimensional nanobeam cavity coupled to a SiN ring resonator.

4. EXPERIMENTAL DESIGN

Given the optimal parameters for the operation of our system, we propose as c_1 an on-substrate SiN cavity with a one dimensional nanobeam structure, with state of the art $V_{eff} \approx 1.2$ and $Q_1 = 6 * 10^4$. Our second cavity has no constraint on V_{eff} however requires a sufficiently large Q_2 which can be accomplished with a SiN ring resonator with $Q_2 = 2 * 10^6$ (9).

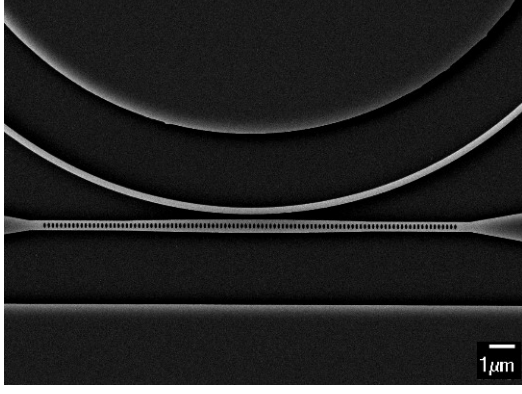


Figure 5. Image of the design gap between c_1 and c_2 determining the coupling coefficient J .

Figure 4. is a graphical representation of the proposed experimental design utilizing a nanobeam cavity and coupled ring resonator. For optimal performance a coupling of $J = 2.1\gamma$ is achieved by engineering an appropriate distance between both resonators, as seen in Figure 5.

Acting as our quantum emitter, colloidal quantum dots QDs are characterized by their constant decay time $\tau = 4.8ns$ and a line width in wavelength $\Delta\lambda = 23nm$. We use both of these values to then calculate the associated dephasing rates

$$\Gamma = \frac{\omega_0^2 \Delta\lambda}{2\pi c} \quad (3)$$

$$\gamma = \frac{1}{\tau}; \quad \gamma^* = \Gamma - \gamma \quad (4)$$

where ω_0 is the emission frequency corresponding to $\lambda = 630nm$.

This then allows us to find the coupling g given the expression (8)

$$g = E_0 \sqrt{\frac{\mu^2 \omega_0}{2\hbar \epsilon_{SiN} \epsilon_0 V_{eff}}} \quad (5)$$

where here $E_0 = 0.35$ (10) the relative strength of the electric field at our emitter and $\mu \approx 50D$ (11) the dipole moment of our emitter.

Finally we also incoherently pump our emitter with a $3ps$ pulse with an amplitude of $P_0 = 120\gamma$. Simulating our system we find a final $I = 0,629$ and a $\beta = 0.152$.

Category	Self-assembled QD in a single cavity	SiV center in coupled cavities	Colloidal QD in coupled cavities (optimal)	Colloidal QD in coupled cavities (experimental)
γ^*/γ	117	2500	83000	83000
$Q_1 \& Q_2$	$\sim 5 \times 10^4$	$7 \times 10^3 \& 5 \times 10^2 / 3.6 \times 10^3 \& 5 \times 10^4$	$6 \times 10^4 \& 2 \times 10^4$	$6 \times 10^4 \& 2 \times 10^4$
$V_{eff,cav}$	$\sim (\lambda/n)^3$	$0.007(\lambda/n)^3$	$0.1(\lambda/n)^3$	$1.2(\lambda/n)^3$
Indistinguishability	~ 0.6	0.94/0.78	0.9	0.63
Efficiency	12.1%	0.26%/0.99%	0.24%	0.15%

Figure 6. Comparison of dephasing, quality factor requirements, mode volume, indistinguishability and efficiency for different optical cavity systems.

5. COMPARISON AND CONCLUSION

Given the results of our simulated system, we compare this with other results for quantum emitters coupled to optical cavities (Table 1.).

In column one, we see the results for a single optical cavity with enhanced I but low β (3). In our second column we see the initially suggested system utilizing two coupled cavities using SiV centers (5), achieving both improved I and β . Finally, the last two columns represent the behaviour of our system first using optimal parameters and second those determined to be experimentally feasible.

Clearly the proposed system for SiV centers predicts the highest joint performance for I and β . However, this system also suffers from the drawback that it requires an extremely low $V_{eff} \approx 0.0005$ (2) which has only been shown using high refractive index material platforms, which is partially absorptive at the SiV resonant frequency (1). Therefore our system produces both improved I and β while remaining experimentally feasible with currently available technology.

I am extremely grateful to Abhi Saxena, for whom this work dominantly belongs. To Arka Majumdar, Gray Rybka, Subhadeep Gupta and the entire REU team/participants.

REFERENCES

- [1] A. Saxena, Y. Chen, A. Ryou, C. G. Sevilla, P. Xu, and A. Majumdar, "Improving indistinguishability of single photons from colloidal quantum dots using nanocavities," *arXiv preprint arXiv:1908.07588*, 2019.
- [2] S. Takeda and A. Furusawa, "Toward large-scale fault-tolerant universal photonic quantum computing," *APL Photonics*, vol. 4, no. 6, p. 060902, 2019.
- [3] T. Grange, G. Hornecker, D. Hunger, J.-P. Poizat, J.-M. Gérard, P. Senellart, and A. Auffeves, "Cavity-funneled generation of indistinguishable single photons from strongly dissipative quantum emitters," *Physical review letters*, vol. 114, no. 19, p. 193601, 2015.
- [4] L. Lanco and P. Senellart, "A highly efficient single photon-single quantum dot interface," in *Engineering the Atom-Photon Interaction*, pp. 39–71, Springer, 2015.
- [5] H. Choi, D. Zhu, Y. Yoon, and D. Englund, "Cascaded cavities boost the indistinguishability of imperfect quantum emitters," *Physical review letters*, vol. 122, no. 18, p. 183602, 2019.
- [6] B. W. Shore and P. L. Knight, "The jaynes-cummings model," *Journal of Modern Optics*, vol. 40, no. 7, pp. 1195–1238, 1993.
- [7] H.-P. Breuer, F. Petruccione, *et al.*, *The theory of open quantum systems*. Oxford University Press on Demand, 2002.
- [8] P. E. Barclay, *Fiber-coupled nanophotonic devices for nonlinear optics and cavity QED*. PhD thesis, California Institute of Technology, 2007.
- [9] E. S. Hosseini, S. Yegnanarayanan, A. H. Atabaki, M. Soltani, and A. Adibi, "High quality planar silicon nitride microdisk resonators for integrated photonics in the visiblewavelength range," *Optics express*, vol. 17, no. 17, pp. 14543–14551, 2009.
- [10] Y. Chen, A. Ryou, M. R. Friedfeld, T. Fryett, J. Whitehead, B. M. Cossairt, and A. Majumdar, "Deterministic positioning of colloidal quantum dots on silicon nitride nanobeam cavities," *Nano letters*, vol. 18, no. 10, pp. 6404–6410, 2018.
- [11] R. Kortschot, J. Van Rijssel, R. van Dijk-Moes, and B. Erne, "Equilibrium structures of pbse and cdse colloidal quantum dots detected by dielectric spectroscopy," *The Journal of Physical Chemistry C*, vol. 118, no. 13, pp. 7185–7194, 2014.